Site-directed placement of three-dimensional DNA origami

Irina Martynenko
Ludwig Maximilian University of Munich
Elisabeth Erber
Ludwig Maximilian University of Munich
Veronika Ruider
Ludwig Maximilian University of Munich
Mihir Dass
Ludwig Maximilian University of Munich
Xin Yin
Ludwig Maximilian University of Munich
Gregor Posnjak
Ludwig Maximilian University of Munich
Philipp Altpeter
Ludwig Maximilian University of Munich
Tim Liedl (tim.liedl@physik.lmu.de)
Ludwig Maximilian University of Munich https://orcid.org/0000-0002-0040-0173

Article

Keywords:

Posted Date: January 27th, 2023

DOI: https://doi.org/10.21203/rs.3.rs-2471674/v1

Version of Record: A version of this preprint was published at Nature Nanotechnology on August 28th, 2023. See the published version at https://doi.org/10.1038/s41565-023-01487-z.

Abstract

Assembling hybrid substrates with nanometer-scale precision and molecular addressability enables advances in such distant fields as material research and biosensing. As such, the combination of lithographic methods with 2D DNA origami self-assembly has led, among others, to the development of photonic crystal cavity arrays and the exploration of sensing nanoarrays where molecular devices are patterned on the sub-micron scale. Here we extend this concept to the third dimension through mounting 3D DNA origami onto nano-patterned substrates followed by silicification to provide mechanical and chemical stability. Our versatile and scalable method relying on self-assembly at ambient temperatures offers the potential to 3D-position any inorganic and organic components that are compatible with DNA architectures. This way, complex and 3D-patterend surfaces designed on the molecular level while reaching macroscopic dimensions could supersede energy-intensive manufacturing steps in substrate processing.

Introduction

Substrates and surfaces structured on the micron and nanometer scale are ubiquitous in modern life and are used in information technology, bio-sensors, water repellent surfaces or cloth and solar cells. To achieve three-dimensional (3D) architectures in chip technology, for example, multiple lithography steps are executed on top of each other. Replacing top-down lithography in parts or entirely through self-assembly processes could help to reduce production times and energy costs. Structural DNA nanotechnology and in particular DNA origami self-assembly[1, 2] has proven useful in the bottom-up fabrication of well-defined complex designer two-dimensional and three-dimensional nanostructures with single-nanometre feature resolution[3, 4, 5, 6, 7, 8, 9]. DNA origami-assisted lithographic methods can successfully transfer spatial information of discrete DNA origami shapes[10, 11, 12, 13, 14, 15] or extended 3D periodic DNA lattices[16] into inorganic substrates. Recently, micrometer-scale periodic 3D DNA patterns assembled from DNA bricks[17] were transferred to Silicon *via* reactive ion etching, successfully reaching line pitches as small as 16.2 nm, which is already smaller than what is achievable with state-of-the-art quadruple patterning or extreme-ultraviolet lithography[16].

Much of the power of DNA origami lies in its ability to serve as a molecular breadboard for positioning molecules and nanoparticles in space with sub-nm precision[18, 19, 20, 21, 22, 23]. By combining DNA origami self-assembly with lithographic nanopatterning, Kershner et al. established so-called DNA origami placement (DOP), a technique based on site- and shape-selective deposition of DNA origami objects onto lithographically patterned substrates, creating large-scale arrays of precisely placed DNA structures[24]. DOP overcame some of the drawbacks mentioned above and demonstrated the ultimate power of dictating the nanoscale arrangement of nanocomponents such as metallic nanoparticles[25], organic dyes[26, 27], proteins[28] and peptides[29] over 2D arrays and patterns. Planar triangular or disc-shaped DNA origami were positioned on substrates patterned by e-beam lithography with very high accuracy and orientation control[27, 30]. To further circumvent the complex e-beam steps in this patterning procedure,

highly parallel and low-cost methods such as self-assembling nanosphere lithography[31, 32, 33] or nanoimprint lithography[30, 34] of centimeter-sized substrates were recently applied. However, all DOP methods developed so far are limited to planar DNA origami and can fabricate 2D arrays and patterns only.

Herein, we demonstrate site-directed placement of various 3D DNA origami shapes in nanometer-precise patterns over micro- to millimeter scales. We employed two different approaches to achieve the upright positioning of various DNA origami shapes via connector-mediated binding (hollow tubes) or direct binding (barrels, tetrapods) via self-aligning. Both approaches are compatible with the two nanopatterning techniques that we tested, e-beam lithography and nanosphere lithography. To mechanically and chemically stabilize the arrays, the DNA structures were silicified on their respective substrates resulting in hybrid DNA–silica structures with controllable heights up to 50 nm and a feature size down to ~ 6 nm. Finally, as a proof of concept, we connected the individually placed DNA origami in the *xy*-plane with further DNA struts in order to create continuous periodic networks.

Main

The various steps of the fabrication process are illustrated in Fig. 1. We deposited 3D DNA origami shapes, which were designed *in-silico*[35, 36] and folded in buffer containing $MgCl_2$ (Fig. 1a), on patterns of hydrophilic binding sites on hydrophobic substrates (Fig. 1b). We adapted protocols described by Gopinath et al. for placing planar DNA origami on such patterned surfaces, which can be produced with e-beam lithography[24] or nanosphere lithography[32]. Effectively, both methods result in a hydrophobic surface with hydrophilic spots which act as the binding sites for the origami structures; we hypothesize primarily for the highly charged phosphate backbone of the DNA. We therefore employed two approaches to achieve upright placement of 3D DNA shapes: i) our hollow nanotubes, for example, have a small footprint in the desired upright position. In the undesired flat-lying orientation, in contrast, such a DNA tube exhibits a large contact area with the hydrophilic spots. Indeed, we observed mostly flat-lying tubes if they were administered directly onto the pre-patterned surfaces. We thus used a two-step process where planar DNA origami sheets were deposited first as connectors and the 3D DNA structures were annealed to these connector sheets in a subsequent step (Fig. 1c). For this, specific anchor strands extend from the ends of the tubes and bind to strands protruding from the planar connector origami sheets. ii) Our barrels are designed such that the bottom-to-be faces of the structure are larger than its side and are therefore more likely to attach to the hydrophilic regions. Or, as in the case of the tetrapod, the four main faces are identical. These two objects were deposited directly on the patterned substrates (Fig. 1d). After successful deposition, samples from both approaches can optionally be incubated with pre-hydrolyzed N-trimethoxysilylpropyl-N,N,N-trimethylammonium chloride (TMAPS) and tetraethylorthosilicat (TEOS) enabling the growth of a rigid silica shell to allow for drying of the products[37] (Fig. 1e).

The two-step placement method, which is based on sequence-specific DNA binding on a surface, enables us to position any 3D DNA origami shape in a defined directionality. As an example shape, we designed a

DNA origami nanotube with a length of 50 nm and a diameter of 40 nm (Fig. 2a). Here, a rolled-up single layer of 48 DNA duplexes forms the tube (Supplementary Note 1, Fig. S1 and Table S1). Its native wall thickness is defined by the width of a DNA double helix, i.e. 2.1 nm. Figure 2a displays a computer graphic of the tube and its built-in binding strands as well as the connector sheet. We used a variant of the “Rothemund triangle”. For one, this is a commonly used origami structure present in many laboratories and second, it has been positioned on lithographically patterned substrates successfully before[30]. Single-stranded DNA linkers extend from the center of the triangle roughly matching the circular footprint of the DNA tube[8]. Hybridization between these linkers and complementary anchor strands extending from the tube’s ends – we labeled both ends of the tubes with anchor strands to increase the probability of binding – brings the tubes and the triangles together in a way that the tubes “stand” on top of the triangles (Fig. 2d, Supplementary Note 2, Fig. S2). Figures 2b through 2d display transmission electron microscopy (TEM) images of the DNA objects where panel b shows a side view of a tube lying flat on the TEM grid, panel c the triangle and panel d the tube assembled on top of a triangle (additional TEM characterization in Fig. S3).

We fabricated Si/SiO_2 chips with square arrays of triangular binding sites situated 250 nm apart from each other *via* e-beam lithography. We deposited DNA triangles, carrying 27 ssDNA linkers each 12 nt in length, on a surface of patterned chips. Generally, the mechanisms of origami-to-site binding are complex and small details in variations during the substrate fabrication can affect placement yields significantly[30]. The experimental conditions for high-quality positioning of planar origami on Si/SiO_2 substrates (Tris buffer, pH of 8.35, Mg^{2+} concentration of 35 mM, incubation time of 1h at RT, see Table S2 for all of the buffers used in the work) have been already reported in ref.[30]. In order to reproduce the successful placement of triangles, we used these parameters and only adjusted the size of the binding sites and the DNA origami concentration (Supplementary Note 3). We achieved up to ~ 94% of sites occupied with a single triangle and ~ 5% of sites with multiple/aggregated triangles (Fig. S4).

Next, we incubated these pre-patterned surfaces with DNA tubes bearing 48 ssDNA anchors each 11 nt in length and complementary to the linker DNA on the triangles at 37°C for 1h in a Tris buffer with 12.5 mM $MgCl_2$ (see Supplementary Note 4.1, Fig. S5, S6 for details on in-solution assembly optimization and Supplementary Note 4.2, Fig. S7-S10 for details on on-surface optimization). After annealing, the chips with the full assemblies were exposed to a silica-coating procedure described in ref.[37]. Subsequent air-drying and AFM and SEM imaging revealed rigid 3D DNA-silica nanotubes arranged in square arrays on the Si/SiO_2 surface (Fig. 2f). We observed up to 75% occupancy of binding sites with individual standing tubes while the remaining 25% of sites were either doubly occupied (4%), empty (2%) or occupied with higher order aggregates (Fig. S10- S13). The height of the silicified tube determined by AFM is ~ 45 nm, which is in good agreement with the designed tube length of ~ 50 nm. The wall thickness of the upright silica-DNA tubes is 6 ± 1 nm, as determined by SEM (insert in Fig. 2i, Fig. S14). This is below the state-of-the-art 10 nm resolution in 3D silica nanofabrication achievable by focused ion beam or thermal scanning probe lithography[38, 39].

Next, we studied how pattern diversity affects the placement and annealing yields. It was shown before that binding of triangles can be a function of array period, especially for binding sites located towards the center of a given array. Occupied sites may inhibit the 2D diffusion of unbound DNA objects to unoccupied sites and so the occupation rate decreases as the period decreases[30]. We examined triangles binding to sites in square arrays with periods ranging between 170 nm and 400 nm on the same Si/SiO_2 chip. To our delight, we did not observe the expected drop of binding rates with a decrease of period from 400 nm to 170 nm (Fig. 3a,c, Fig. S15). In fact the highest percentage of 95% of sites binding a single triangle for the 250 nm period is slightly decreased to 93% for the 400 nm period and to 91% for the 170 nm period. Consequently, the site occupancy and alignment of standing tubes in arrays of corresponding periods did not vary significantly. We achieved up to 71% and 74% of sites with individual upright nanotubes for the 170 nm and 400 nm arrays, respectively (Fig. 3, b-d, f-h, Supplementary note 5, Fig. S16). This opens a route to create diverse patterns and arrays of integrated 3D DNA-silica nanodevices on one chip.

For many applications it can be advantageous to use a cleanroom-free, large-scale DNA origami placement method such as the benchtop technique of nanosphere-DNA origami lithography described in ref.[32]. In nanosphere lithography, a layer of close-packed nanospheres creates a crystalline pattern of contact points for the selective passivation of the supporting glass substrate[32]. After chemically rendering the “free” glass surface hydrophobic, the nano-spheres are lifted off and DNA origami structures can subsequently bind to the hydrophilic, close-packed, hexagonal pattern defined by the previous contact points.

We utilized this method of bottom-up nanopatterning for the two-step placement described above. Although nanosphere lithography creates circular binding sites, we achieved similar success in triangle placement as Shetty et al.[32] did with circular DNA origami (Fig. 3i, Fig. S17). The yield of single tubes attaching to the triangles increased with the incubation time (Fig. S18), but it never came close to the values obtained for e-beam lithography patterning on Si/SiO_2 chips. After 3 h of annealing at 37°C, the occupancy of sites reached ~ 78% with only ~ 35% of sites carrying a single standing tube. Further incubation (up to 24 h) leads to almost full occupancy of the binding sites (~ 97%), however, with still only ~ 36% of sites with single tubes accompanied by a dramatic increase in multiple binding events. This could be a result of the geometrical mismatch between the circular biding sites and the triangular DNA origami connectors, which leaves free hydrophilic binding space where the DNA tubes can bind directly. Noteworthy, our hexagonal arrays of sphere-lithography assembled DNA tubes cover a total area of more than 4 mm^2 (Fig. S19), proving that it is possible to arrange complex 3D DNA-silicified molecular breadboards over macroscopic areas in a conventional wet lab environment.

Another approach to binding the 3D origami shapes to substrates relies on direct binding and self-aligning. To achieve this, it is necessary to either design the objects such that certain faces are more likely to attach to the hydrophilic binding sites or that all main faces are identical.

As an example of the first case, we demonstrate upright positioning of DNA origami barrels. Our DNA origami barrel is a donut-shaped structure designed previously [9] and constructed from horizontally aligned, circular DNA duplexes. The barrel has a diameter of 60 nm and a height of 27 nm (Fig. 5a-c, Fig. S20). The relatively thick walls and a low aspect ratio of 1:2.2 (height to width) promote the horizontal binding of the structures. Moreover, the binding sites were tuned to match the diameter of the barrels. We fabricated a series of Si/SiO_2 chips *via* e-beam lithography with circular binding sites, varying the diameter between 75% and 200% of the actual barrel diameter of 60 nm. We obtained the best yield of single bound upright barrels (70%) with spot sizes of 45 nm while the percentage of the barrels lying on side is reduced to 16% (Fig. 4d,e and Supplementary Note 6, Fig. S21-S24).

As an example of the second design case, we employed a DNA origami tetrapod that consists of four equivalent arms, resulting in a four-fold symmetric object (Fig. 4f, g and Fig. S25, S26). Each arm is composed of interconnected 24-helix bundles (24HBs) as described in Supplementary Note 7. As expected, after incubating the origami tetrapods on patterned substrates, we observed individual objects standing on three legs on the binding sites (Fig. 5f). After optimization of binding site shape and size, we achieved occupancy yields of 79% while single therapods occupied 43% of the sites and 36% of the sites carried multiple tetrapods (Supplementary note 8, Fig. S27-S29). Square arrays with a 200 nm period of silica coated and dried tetrapods imaged by SEM and AFM are presented in Fig. 4h and i, respectively. The height of an individual silica-coated tetrapod obtained from AFM measurements of dried samples is ~ 40 nm, which is in fair agreement with the designed 50 nm. Most likely, the tetrapod “sits” flat on the surface, reducing the effective height of the structures. We assume that a similar approach can be used for the individual placement of all 3D shapes with equilateral faces such as tetrahedrons, cubes, octahedrons, etc. Overall, while the arrangement of deposited 3D structures in this one-step method is worse compared to the two-step process, it can be helpful for positioning a large variety of 3D shapes with low-aspect ratio as cuboids, cylinders or cones.

Individually placed 3D DNA shapes can be used as seeds for further assembly in subsequent surface annealing steps. Both the DNA shapes and the lithographic pattern can be rationally designed to create not just periodic arrays but complex 3D networks. As a proof-of-concept, we created large-scale periodic honeycomb networks by a 2-step placement procedure with the initial placement of tetrapods followed by the annealing of 24 HBs to the legs of the tetrapods (Fig. 5a,). Here, tetrapods bearing 12 ss-DNA linkers on each leg were deposited to the nodes of the lithography-patterned honeycomb array (Fig. 5b). We adjusted the spacing between neighboring tetrapods (i.e. the lengths of edges of the hexagons) to 170 nm to accommodate a 24HB with 12 complementary anchor strands extending from both sides (Fig. 6c, Supplementary notes 9 and Fig. S30). After the surface annealing, each 24HB interconnects a pair of neighboring tetrapods, thus forming the edges of the hexagons (Fig. 6c, d). During the annealing step the tetrapods reorient on their binding sites so that three legs of the individual tetrapod align with the directions of the edges of the hexagons. The resulting network is designed as a micron-sized honeycomb array (Fig. 6d) or as a fractal arrangement of individual hexagons forming a Sierpiński triangle (Fig. 6e, Fig. S31b).

In conclusion, we advanced from 2D to 3D in the placement of individual origami objects on lithographically defined surfaces. In addition to reducing multiple bindings per site and the number of empty binding spots, we achieved full control over the face-oriented binding of our 3D DNA origami shapes. With the help of wet-chemistry-coating we were able to build hybrid DNA–silica structures with controllable heights up to 50 nm and a feature size down to ~ 6 nm covering large-scale arrays. Moreover, and importantly for future applications of such DNA-assembled 3D substrates, nanometer-precise modification with a wide variety of nanoscale components can be directly implemented on the DNA origami templates. Individual placement of 3D DNA origami on macroscopic patterns could complement conventional methods of lithographic shaping of diverse materials for the site-directed organization of matter at nanoscale. We envision that these strategies will entail unprecedented freedom of design and versatility into 3D nanofabrication.

Methods

DNA Origami design, preparation and purification

DNA origami nanotubes and tetrapods were designed using caDNAno[35]. Design details of the DNA nanotube can be found in Supplementary Note 1. Design details of tetrapods and 24HBs can be found in Supplementary Note 7 and Supplementary Note 9, respectively.

Staple strands were purchased from IDT Technologies (HPLC purified, 100 µM each in water). The scaffold strands (p7249, p8634) were produced from M13 phage replication in Escherichia coli. All chemicals were obtained from Sigma Aldrich unless otherwise stated. DNA origami structures used in this work (nanotubes, triangles, barrels, tetrapods and 24HB) were folded by mixing scaffold strands with an excess of staple strands (and miniscaf short scaffold-parity strands in case of DNA origami barrels) in Folding buffer (buffers used in this work can be found in Supplementary Table 2). Samples were annealed in a PCR machine (Tetrad 2 Peltier thermal cycler, Bio-Rad) and purified from excess staples by Amicon filtration[40] (triangles, nanotubes), PEG precipitation[41] (tetrapods, 24HB) or ultracentrifugation[42] (barrels). A full description of the folding and purification of each type of DNA origami can be found in Supplementary Note 10.

Annealing of DNA origami in buffer solution

For the triangular origami, 9, 18, or 27 staples close to the central hole were modified by extending 8, 12 or 20 nt polyA sequences from the 5' end (Fig. S2). These A_8, A_{12}, A_{20}-modified DNA staples were introduced into the DNA scaffolds in place of the original DNA staples. After folding, excess staples were removed by filtering the DNA origami solution through 0.5 mL Amicon 100 kDa filter units.

For the nanotubes, 24 staples on each edge of a tube were modified by extending 11 nt polyT sequences from the 3' end (Supplementary Note 2 and Fig. S2). These T_{11}-modified DNA staples were introduced into the DNA scaffolds in place of the original DNA staples and folded and purified as described in Supplementary Note 10.

The binding of T-modified DNA nanotubes to A-modified DNA triangles in suspension was studied at a final concentration of tubes and triangles of ~5 nM and optimized by varying the length and number of linkers. The solutions were mixed in the Placement buffer (Table S2) in 50 µl aliquots, annealed 1 h either at 37°C in the thermal cycler or at room temperature, and imaged by gel electrophoresis and TEM.

Preparation of the substrates and DNA origami placement

Patterned Si/SiO_2 substrates were prepared by adaptation of procedure from ref.[30] with slight modification. Patterned glass substrates were prepared following the protocol reported in ref.[32]. All steps were carried out in a cleanroom. Step by step protocols of preparation of the patterned substrates and placement of DNA origami can be found in Supplementary Note 11 and Supplementary Note 12, respectively.

Characterization techniques and data analysis

UV-vis absorption measurements were performed with a NanoDrop ND-1000 Spectrophotometer (Thermo Scientific).

Tapping-mode AFM of dried Si/SiO_2 or glass substrates with triangular DNA origami was carried out on a Dimension ICON AFM (Bruker). OTESPA silicon tips (300 kHz, Vecco Probes) were used for imaging in air. Images are analysed with the Software Gwyddeon. We measured binding site occupancy (percentage of sites with one or more triangular origami) by hand-annotating the AFM images as shown in Fig. S4a. For e-beam lithography on Si/SiO_2, we analyzed 300 binding sites for each of three independent replications of the experiment (of the Si/SiO_2 substrate preparation, placement, washing, etc.). The number of sites analyzed per replicate depended on the array period — 300 sites were analyzed for 170 nm and 250 nm period but only 144 sites were analyzed for 400 nm period. For the nanosphere lithography on glass, 600 binding sites in the middle of the glass were analyzed in a single experiment.

TEM imaging of DNA origami lattices was carried out using a JEM-1011 transmission electron microscope (JEOL) operating at 80 kV. For sample preparation 5 ul of DNA origami diluted to 5 nM concentration were deposited on glow-discharged TEM grids (formvar/carbon-coated, 300 mesh Cu; TED Pella, Inc; prod no. 01753 - f) for 30 sec. Grids were furthermore quickly washed once with 1% uranyl formate solution (5 µL) and immediately afterwards stained with another 5 µL drop of uranyl formate for 10 s.

The Scanning Electron Microscope used in this work is the Raith e-LiNE Scanning Electron Microscope (Raith). The beam settings for imaging are 10 kV acceleration and 20 µm aperture. Samples were SEM imaged after 30 s sputtering using an Edwards Sputtercoater S150B 1990. The sputter target contained 60% gold and 40% palladium. Process parameters used for sputtering were 5 mbar Ar, 1.5 kV, 11 mA. 30 s sputtering results in the deposition of layer of gold/palladium with a thickness of a few nm. SEM imaging of the samples was performed on horizontal samples and samples tilted by 70 . We measured binding site occupancy (percentage of sites without origami, or with one or more origami) and alignment (in

upright or on-site position) of DNA origami triangle-nanotubes structures, barrels and tetrapods by hand-annotating the top-view SEM images, as shown in Fig. S7, Fig. S21 and Fig. S27, respectively. For e-beam lithography on Si/SiO_2, we typically analyzed 600 binding sites for each of two independent replications of the experiment. For the optimization of triangle-nanotube binding on a surface and barrel placement we performed only single replication of experiments. Nanotube placement yields on glass were counted in the middle of the glass and on 2 separated spots each approximately 1 mm apart from the middle point.

Declarations

DETAILS ON AUTHORS CONTRIBUTIONS

T.L. and I.M. designed this study. I.M., E.E. and V.R. designed, assembled, purified DNA origami samples, designed and optimized interfaces. G.P. and X.Y. designed, assembled, purified DNA origami tetrapods and 24HBs and designed the tetrapod-24HB interface. I.M., E.E., V.R. and M.D. performed placement experiments, surface annealing experiments, AFM and SEM measurements and data analysis with the assistance from P.A.. I.M. and T.L. wrote the manuscript with input from all authors.

COMPETING INTERESTS

The authors declare no competing financial interest.

ACKNOWLEDGMENTS

We thank Christian Obermayer for clean room assistance and Susanne Kempter for assistance with TEM. We thank all members of Tim Liedl Group for the helpful discussions. I.M., E.E., G.P. and T.L. acknowledge funding from the ERC consolidator grant “DNA Funs” (Project ID: 818635) V.R., X.Y. and T.L. further acknowledge support from the cluster of excellence e-conversion EXC 2089/1- 390776260. This work was funded by the Federal Ministry of Education and Research (BMBF) and the Free State of Bavaria under the Excellence Strategy of the Federal Government and the Länder through the ONE MUNICH Project Munich Multiscale Biofabrication.

ONLINE CONTENT

Supplementary information, additional references, can be found online

DATA AVAILABILTY STATEMENT

All relevant data generated or analysed during this study are included in this published article (and its supplementary information files). Electron microscopy and AFM images of replicate samples are available from the corresponding authors on request (tim.liedl@lmu.de, irina.martynenko@physik.lmu.de).

References

1. Rothemund PWK. Folding DNA to create nanoscale shapes and patterns. Nature 2006, **440**(7082): 297–302.
2. Douglas SM, Dietz H, Liedl T, Högberg B, Graf F, Shih WM. Self-assembly of DNA into nanoscale three-dimensional shapes. Nature 2009, **459**(7245): 414–418.
3. Seeman NC. DNA in a material world. Nature 2003, **421**(6921): 427–431.
4. Yan H, Park SH, Finkelstein G, Reif JH, LaBean TH. DNA-templated self-assembly of protein arrays and highly conductive nanowires. Science 2003, **301**(5641): 1882–1884.
5. Aldaye FA, Palmer AL, Sleiman HF. Assembling materials with DNA as the guide. Science 2008, **321**(5897): 1795–1799.
6. Wang P, Huh J-H, Lee J, Kim K, Park KJ, Lee S, *et al.* Magnetic Plasmon Networks Programmed by Molecular Self-Assembly. Adv Mater 2019, **31**(29): 1901364.
7. Liu X, Zhang F, Jing X, Pan M, Liu P, Li W, *et al.* Complex silica composite nanomaterials templated with DNA origami. Nature 2018, **559**(7715): 593–598.
8. Sun W, Boulais E, Hakobyan Y, Wang WL, Guan A, Bathe M, *et al.* Casting inorganic structures with DNA molds. Science 2014, **346**(6210): 1258361.
9. Kolbeck PJ, Dass M, Martynenko IV, van Dijk-Moes RJ, Brouwer KJ, van Blaaderen A, *et al.* A DNA origami fiducial for accurate 3D AFM imaging. *bioRxiv* 2022.
10. Kabusure KM, Piskunen P, Yang J, Kataja M, Chacha M, Ojasalo S, *et al.* Optical characterization of DNA origami-shaped silver nanoparticles created through biotemplated lithography. Nanoscale 2022, **14**(27): 9648–9654.
11. Diagne CT, Brun C, Gasparutto D, Baillin X, Tiron R. DNA Origami Mask for Sub-Ten-Nanometer Lithography. ACS nano 2016, **10**(7): 6458–6463.
12. Surwade SP, Zhao S, Liu H. Molecular Lithography through DNA-Mediated Etching and Masking of SiO2. J Am Chem Soc 2011, **133**(31): 11868–11871.
13. Jin Z, Sun W, Ke Y, Shih C-J, Paulus GLC, Hua Wang Q, *et al.* Metallized DNA nanolithography for encoding and transferring spatial information for graphene patterning. Nature Communications 2013, **4**(1): 1663.
14. Shen B, Linko V, Tapio K, Pikker S, Lemma T, Gopinath A, *et al.* Plasmonic nanostructures through DNA-assisted lithography. Science Advances 2018, **4**(2): eaap8978.
15. Surwade SP, Zhou F, Wei B, Sun W, Powell A, O'Donnell C, *et al.* Nanoscale Growth and Patterning of Inorganic Oxides Using DNA Nanostructure Templates. J Am Chem Soc 2013, **135**(18): 6778–6781.
16. Shen J, Sun W, Liu D, Schaus T, Yin P. Three-dimensional nanolithography guided by DNA modular epitaxy. Nature Materials 2021, **20**(5): 683–690.
17. Ke Y, Ong LL, Shih WM, Yin P. Three-Dimensional Structures Self-Assembled from DNA Bricks. Science 2012, **338**(6111): 1177–1183.

18. Maune HT, Han S-p, Barish RD, Bockrath M, Iii WAG, Rothemund PWK, *et al.* Self-assembly of carbon nanotubes into two-dimensional geometries using DNA origami templates. Nature Nanotechnology 2010, **5**(1): 61–66.
19. Kuzyk A, Schreiber R, Fan Z, Pardatscher G, Roller E-M, Högele A, *et al.* DNA-based self-assembly of chiral plasmonic nanostructures with tailored optical response. Nature 2012, **483**(7389): 311–314.
20. Voigt NV, Tørring T, Rotaru A, Jacobsen MF, Ravnsbæk JB, Subramani R, *et al.* Single-molecule chemical reactions on DNA origami. Nature Nanotechnology 2010, **5**(3): 200–203.
21. Knudsen JB, Liu L, Bank Kodal AL, Madsen M, Li Q, Song J, *et al.* Routing of individual polymers in designed patterns. Nature Nanotechnology 2015, **10**(10): 892–898.
22. Hartl C, Frank K, Amenitsch H, Fischer S, Liedl T, Nickel B. Position Accuracy of Gold Nanoparticles on DNA Origami Structures Studied with Small-Angle X-ray Scattering. Nano Lett 2018, **18**(4): 2609–2615.
23. Funke JJ, Dietz H. Placing molecules with Bohr radius resolution using DNA origami. Nature Nanotechnology 2016, **11**(1): 47–52.
24. Kershner RJ, Bozano LD, Micheel CM, Hung AM, Fornof AR, Cha JN, *et al.* Placement and orientation of individual DNA shapes on lithographically patterned surfaces. Nature Nanotechnology 2009, **4**(9): 557–561.
25. Hung AM, Micheel CM, Bozano LD, Osterbur LW, Wallraff GM, Cha JN. Large-area spatially ordered arrays of gold nanoparticles directed by lithographically confined DNA origami. Nature Nanotechnology 2010, **5**(2): 121–126.
26. Gopinath A, Miyazono E, Faraon A, Rothemund PWK. Engineering and mapping nanocavity emission via precision placement of DNA origami. Nature 2016, **535**(7612): 401–405.
27. Gopinath A, Thachuk C, Mitskovets A, Atwater HA, Kirkpatrick D, Rothemund PWK. Absolute and arbitrary orientation of single-molecule shapes. Science 2021, **371**(6531): eabd6179.
28. Cervantes-Salguero K, Freeley M, Gwyther REA, Jones DD, Chávez JL, Palma M. Single molecule DNA origami nanoarrays with controlled protein orientation. Biophysics Reviews 2022, **3**(3): 031401.
29. Huang D, Patel K, Perez-Garrido S, Marshall JF, Palma M. DNA Origami Nanoarrays for Multivalent Investigations of Cancer Cell Spreading with Nanoscale Spatial Resolution and Single-Molecule Control. ACS nano 2019, **13**(1): 728–736.
30. Gopinath A, Rothemund PWK. Optimized Assembly and Covalent Coupling of Single-Molecule DNA Origami Nanoarrays. ACS nano 2014, **8**(12): 12030–12040.
31. Deckman HW, Dunsmuir JH. Natural lithography. Appl Phys Lett 1982, **41**(4): 377–379.
32. Shetty RM, Brady SR, Rothemund PWK, Hariadi RF, Gopinath A. Bench-Top Fabrication of Single-Molecule Nanoarrays by DNA Origami Placement. ACS nano 2021, **15**(7): 11441–11450.
33. Martynenko IV, Ruider V, Dass M, Liedl T, Nickels PC. DNA Origami Meets Bottom-Up Nanopatterning. ACS nano 2021, **15**(7): 10769–10774.

34. Penzo E, Wang R, Palma M, Wind SJ. Selective placement of DNA origami on substrates patterned by nanoimprint lithography. Journal of Vacuum Science & Technology B 2011, **29**(6): 06F205.
35. Douglas SM, Marblestone AH, Teerapittayanon S, Vazquez A, Church GM, Shih WM. Rapid prototyping of 3D DNA-origami shapes with caDNAno. Nucleic Acids Res 2009, **37**(15): 5001–5006.
36. Kim D-N, Kilchherr F, Dietz H, Bathe M. Quantitative prediction of 3D solution shape and flexibility of nucleic acid nanostructures. Nucleic Acids Res 2011, **40**(7): 2862–2868.
37. Jing X, Zhang F, Pan M, Dai X, Li J, Wang L, *et al.* Solidifying framework nucleic acids with silica. Nat Protoc 2019, **14**(8): 2416–2436.
38. Wen X, Zhang B, Wang W, Ye F, Yue S, Guo H, *et al.* 3D-printed silica with nanoscale resolution. Nature Materials 2021, **20**(11): 1506–1511.
39. Seniutinas G, Balčytis A, Reklaitis I, Chen F, Davis J, David C, *et al.* Tipping solutions: emerging 3D nano-fabrication/ -imaging technologies. Nanophotonics 2017, **6**(5): 923–941.
40. Shaw A, Benson E, Högberg B. Purification of Functionalized DNA Origami Nanostructures. ACS nano 2015, **9**(5): 4968–4975.
41. Stahl E, Martin TG, Praetorius F, Dietz H. Facile and scalable preparation of pure and dense DNA origami solutions. Angew Chem Int Ed Engl 2014, **53**(47): 12735–12740.
42. Lin C, Perrault SD, Kwak M, Graf F, Shih WM. Purification of DNA-origami nanostructures by rate-zonal centrifugation. Nucleic Acids Res 2012, **41**(2): e40-e40.

Figures

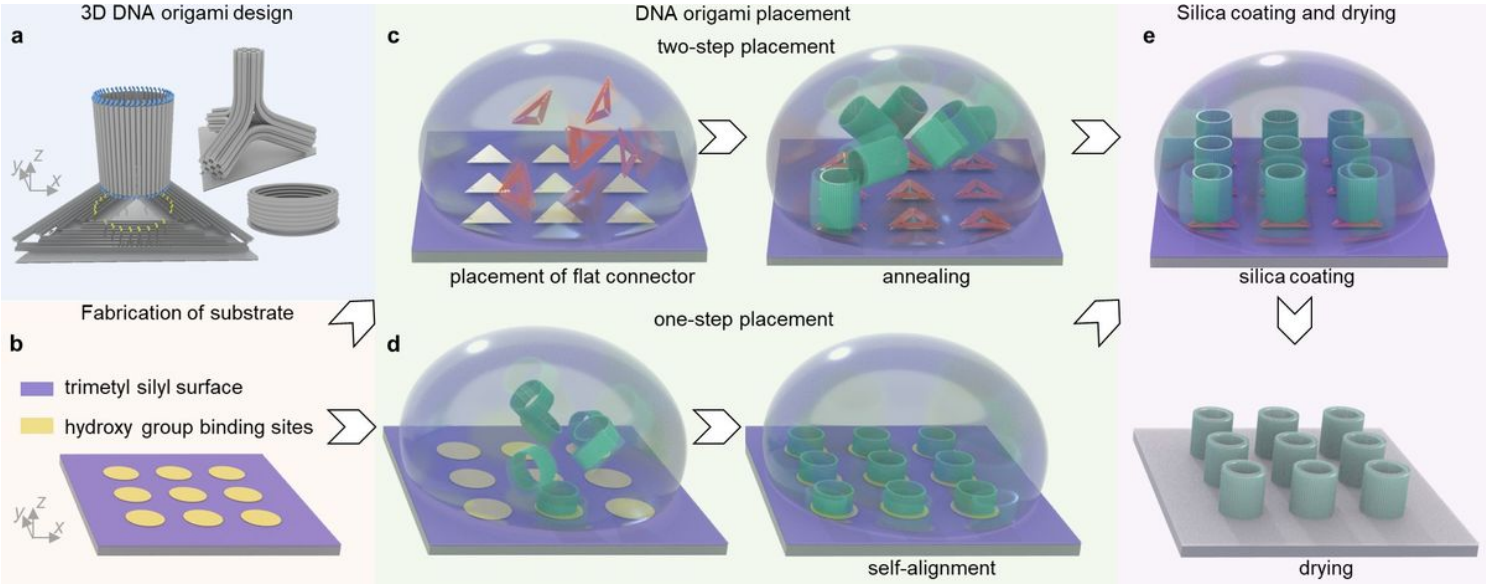

Figure 1

Assembly of 3D hybrid DNA-silica nanostructured substrates. a) Design of 3D DNA origami shapes and connection interfaces for on-surface assembly. b) Substrates are patterned by e-beam[30] or nanosphere

lithography[32] to produce hydrophilic oxide patterns on HMDS-primed hydrophobic background (Si/SiO_2 or glass). c, d) Alignment and upright positioning of 3D DNA origami structures on patterned surfaces. DNA is represented in a cylinder model. Shapes that cannot self-align in an upright position are placed in a 2-step process with planar DNA origami as connectors (Fig. 1c). Other shapes are directly deposited to the patterned substrate (Fig. 1d right). e) Growing rigid silica shells on the 3D DNA origami enables subsequent drying of the now rigidified objects.

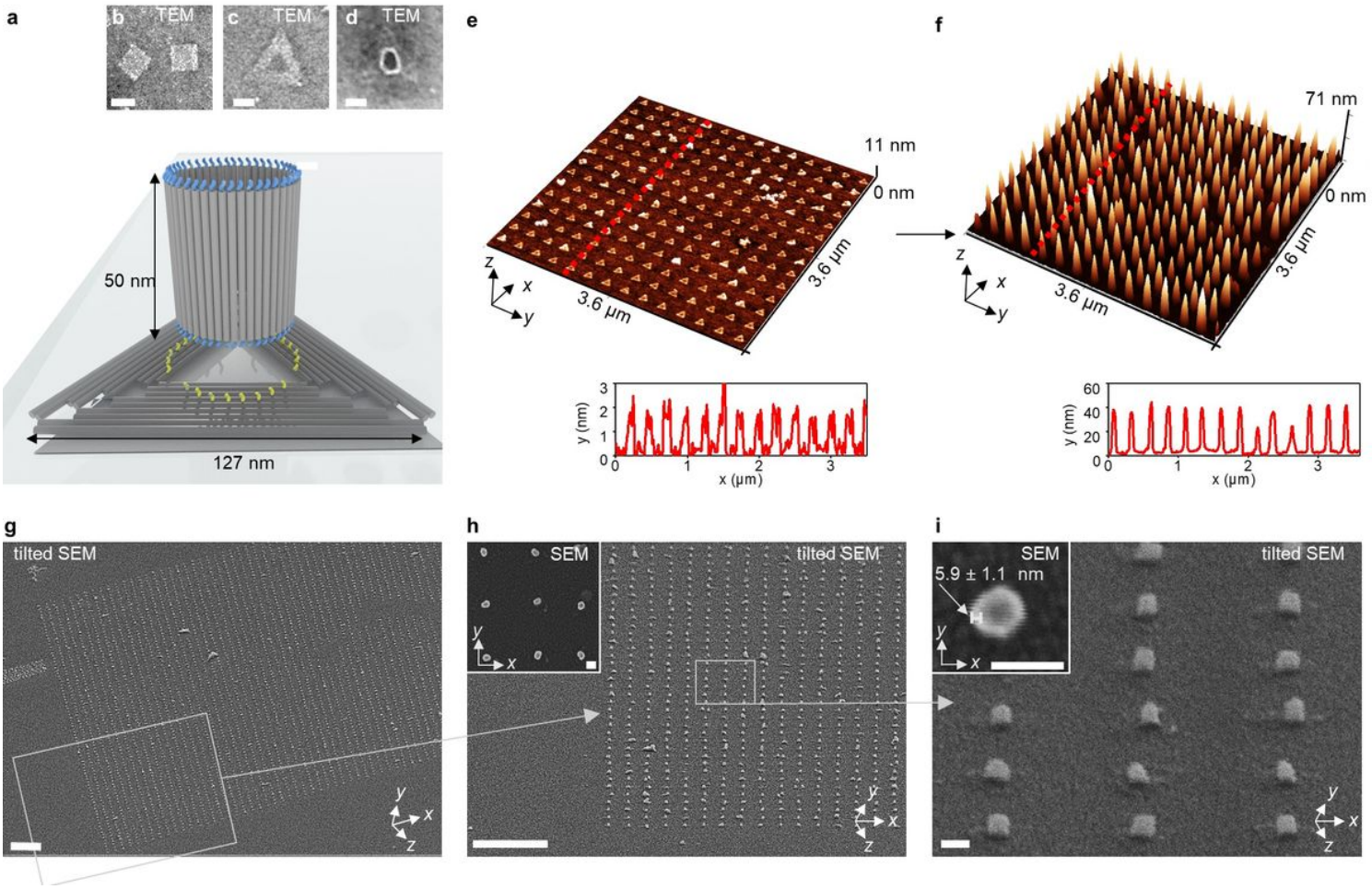

Figure 2

Assembly of 3D hybrid nanostructured substrates by on-surface annealing of DNA origami nanotubes to a flat connector origami. a) Design of the DNA origami tubes and triangles. Single-stranded DNA linkers extend from the center of the triangle roughly matching the circular footprint of the tube. Complementary anchor strands extend from the ends of the tubes. b-d) Uranyl-formate negative-stain TEM images of b) DNA tubes carrying 48 T_{11} ssDNA linkers, c) a triangle, carrying 27 A_{12} ssDNA anchors and d) a tube annealed with a triangle. e) AFM characterization of dried Si/SiO_2 chip with an array of DNA origami triangles carrying 27 A_{12} ssDNA anchors. f) AFM and g-i) SEM characterization of dried Si/SiO_2 chip with an array of silica-coated DNA tubes standing on top of triangles. Scale bars in g) and h): 1 µm. Scale bars in b – d, i) and in the inserts in h, i): 50 nm.

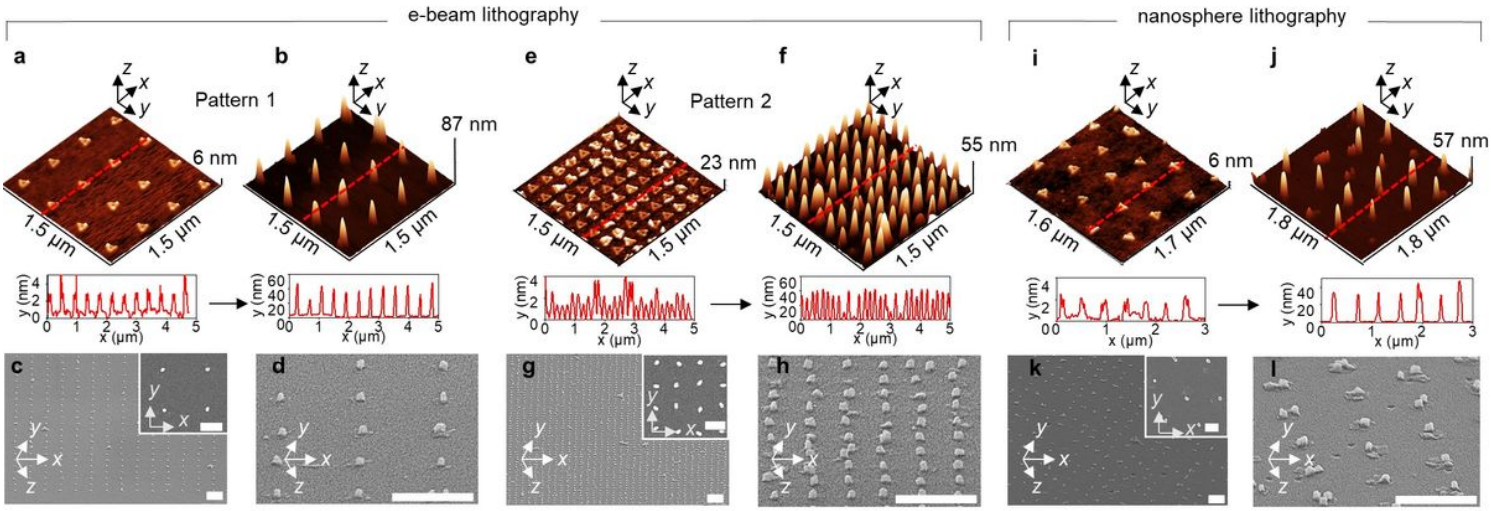

Figure 3

Pattern diversity. a-h) AFM and SEM characterization of dried Si/SiO_2 surfaces with square arrays of DNA origami prepared with e-beam lithography with periods of 400 nm (a-d) and 170 nm period (e-h). a, e) AFM characterization of surfaces with square arrays of DNA origami triangles carrying ssDNA linkers. b, f) AFM and c, d, g, h) SEM characterization of surfaces with arrays of silica-coated DNA tubes standing upright on the triangles. i-l) AFM and SEM characterization of a dried glass surface with a hexagonal pattern of DNA origami prepared *via* nanosphere lithography[32]. i) AFM characterization of the glass surface with a hexagonal array of DNA origami triangles carrying ssDNA linkers. j) AFM and k, l) SEM characterization of dried glass chip with a hexagonal array of silica-coated DNA tubes standing on top of triangles. c, d, g, h, k, l) are tilted SEM images, inserts are top-view SEM images. All scale bars: 400 nm. Scale bars in the inserts in c, g, k): 200 nm.

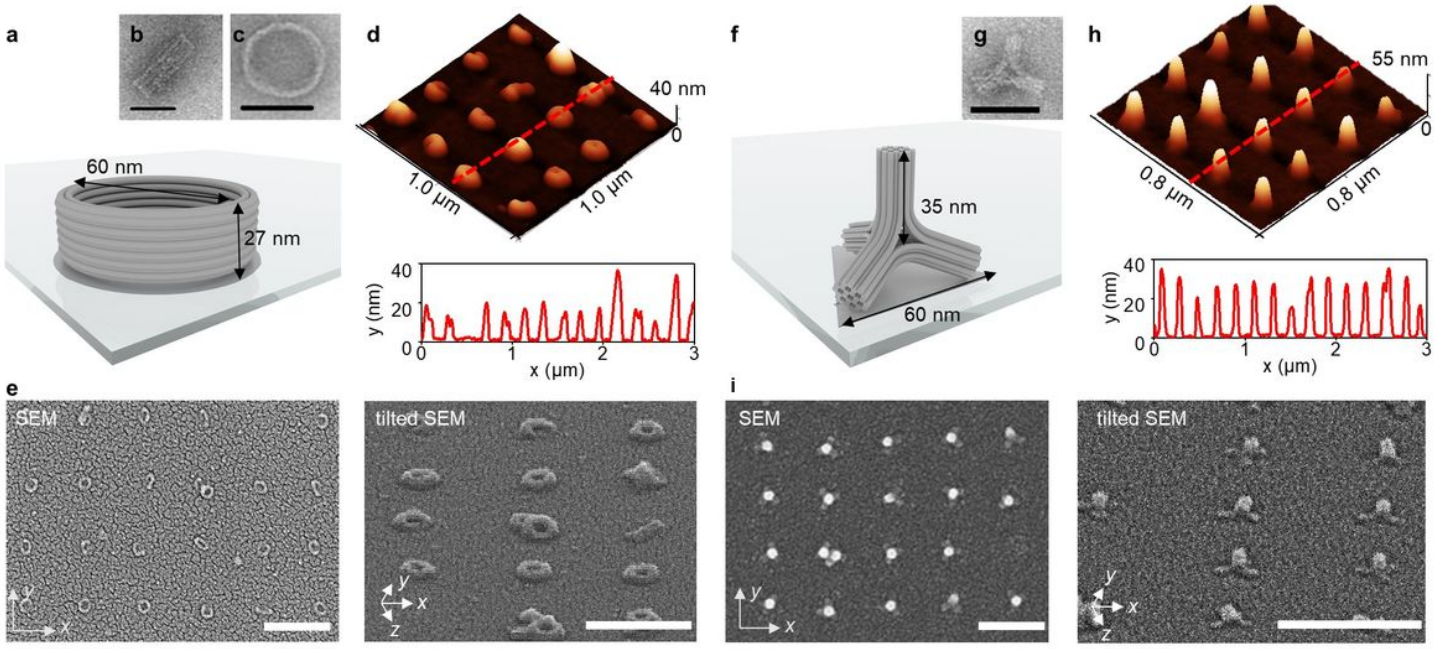

Figure 4

Assembly of 3D hybrid nanostructured substrates by direct deposition. a) Design of the DNA origami barrels, illustrated as a cylinder model. b, c) Uranyl formate negative-stain TEM images of b) a DNA origami barrel lying on its side, c) an upright DNA origami barrel. d, e) AFM and SEM characterization of a dried Si/SiO_2 substrate with a square array of silicified DNA origami barrels. f) Design of the DNA origami tetrapods. g) Uranyl formate negative-stain TEM images of the DNA origami tetrapod. d, e) AFM and SEM characterization of a dried Si/SiO_2 substrate with a square array of silicified DNA origami tetrapods. Scale bars in e, i): 400 nm.

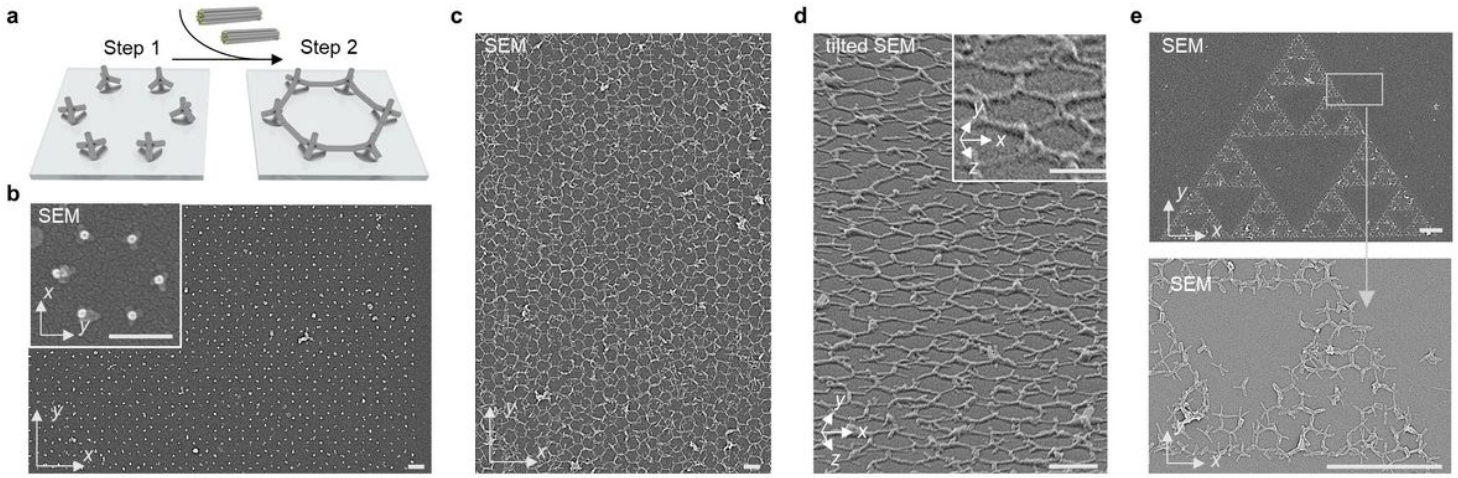

Figure 5

Assembly of 3D hybrid periodic networks on substrates by on-surface annealing of DNA origami 24HBs to the tetrapods, pre-adsorbed on the binding sites. a) Assembly of the periodic networks in a two-step process. First, DNA origami tetrapods adsorb to the binding sites arranged in a honeycomb lattice (Step 1). 24HBs connect neighboring tetrapods pairs in an annealing process (Step 2). b) SEM images of Si/SiO_2 substrate in a honeycomb lattice of tetrapods bearing 12 ss-DNA linkers. c-e) SEM characterization of the same sample as in (b), interconnected with 24HB bearing 12 anchor strands from both sides. The resulting continuous network covers a micron-sized honeycomb pattern (c, d) and can be designed as a fractal arrangement of individual hexagons forming Sierpiński triangle (e). Scale bars in b-d): 400 nm. Scale bars in e): 2 µm.

Supplementary Files

This is a list of supplementary files associated with this preprint. Click to download.

- martynenkoSI.pdf